EPJ Web of Conferences **63**, 01004 (2013)
DOI: 10.1051/epjconf/20136301004

New development of the projected shell model and description of low-lying collective states in transitional nuclei

Fang-Qi Chen[1,a] and Yang Sun[1,2,b]

[1] *Department of Physics and Astronomy, Shanghai Jiao Tong University, Shanghai 200240, People's Republic of China*
[2] *Institute of Modern Physics, Chinese Academy of Sciences, Lanzhou 730000, People's Republic of China*

Abstract. Description of the interplay between different nuclear shapes is an interesting but challenging problem. The original projected shell model (PSM) is applicable to nuclei with fixed shapes. We extend the PSM by superimposing (angular-momentum- and particle-number-) projected product wave functions in the spirit of the generate coordinate method. With this development, the Gd isotopes across the $N = 90$ region are studied, and the results indicate spectroscopic features of shape phase transition with varying neutron number. In order to illustrate the shape distribution in microscopic wave functions, we introduce a deformation representation and show that the collectively excited $K^\pi = 0^+$ states in the Gd isotopes have characters of shape vibration.

1 Introduction

Nuclei are among the few quantum systems where one can discuss them in terms of shape [1]. Different shapes of nuclei correspond to fundamentally different nuclear wave functions that characterize the microscopic motions of nucleons. A large number of nuclei in the nuclear chart can be understood with well-defined shapes, either spherical or deformed. However, there are known cases where more interesting situations can occur, as for instance, coexistence of different shapes within one nucleus [2]. Examples are coexistence of normally-deformed and superdeformed prolate shapes [3, 4] or coexistence of two or more shapes around the spherical equilibrium [5, 6]. Shape changes can also occur as nuclei rotate and several rotation-driving phenomena have been known [7–9].

Description of the above-mentioned observations is a challenging task for nuclear theory. The shapes and shape phase transitions have been mostly discussed either in the geometric framework such as the Bohr model [10], or in the algebraic models such as the interacting boson model [11]. In the geometric aspect, analytical solutions can be obtained at the critical point of the phase transition from the spherical to axially deformed shape by using the Bohr Hamiltonian [10]. In the algebraic models, different shapes are described by different dynamic symmetrical limits, and the critical points can be found on some specific routes from one symmetrical limit to another [12]. In both of the geometrical and algebraic methods, the shape phase transition is controlled by some parameters, which is varied artificially across the phase transitional region.

It is desired that the variation of shapes can be studied from the microscopic point of view. The shape transition in Nd isotopes has been discussed [13] within the relativistic mean-field framework, generalized with the generator coordinate method. In Ref. [13], the phase-transition behavior emerges naturally with increasing neutron number, which can be described simultaneously with other quantities such as excitation spectra and transition probabilities. The advantage of using microscopic methods is that they can provide wave functions from which one can learn about the insight of the system. However, the microscopic wave functions are given in terms of nucleon degrees of freedom, while "shape phases" are usually defined in terms of collective variables. In principle, there is no way to define a "deformation operator" and use its eigenfunctions to expand microscopic wave functions. This means that it is not possible to directly obtain the wave functions in terms of deformation (as those obtained in geometric calculations) by using a simple unitary transformation.

In the present work we report on a new development of the projected shell model [14] by superimposing different intrinsic states corresponding to different deformations. We diagonalize the shell model Hamiltonian by solving the Hill-Wheeler equation [15] in the basis spanned by the angular-momentum- and particle-number-projected states. We propose a transformation for the obtained wave functions to a "deformation representation". The transformation is defined with the generator coordinate method (GCM) by using the quadrupole deformation as the generator coordinate. We give a proof that such a GCM wave function written in a nonorthogonal basis can be transformed into a deformation representation.

In Sect. 2 we present a general transformation that brings the shell-model wave functions into the deformation representation. A brief introduction for the extension of PSM is given in Sect. 3. The calculated examples and

[a] e-mail: fangqi0591@qq.com
[b] e-mail: sunyang@sjtu.edu.cn

their discussions are presented in Sect. 4, and finally in Sect. 5, we draw a conclusion.

2 The deformation representation

We first introduce a transformation of the microscopic wave function

$$|\Psi\rangle = \int f(\epsilon_2)\,|\psi(\epsilon_2)\rangle\, d\epsilon_2 \tag{1}$$

to the *deformation representation*. Equation (1) is a general wave function expressed as a superposition of wave functions corresponding to different deformations. Generally, $|\psi(\epsilon_2)\rangle$ with deformation ϵ_2 is not orthogonal to $\left|\psi(\epsilon_2')\right\rangle$ with another ϵ_2', and therefore, $f(\epsilon_2)$ in (1) is not a proper quantity to represent the probability of deformation. Assuming that we could define a set of states $|\epsilon_2\rangle$ with definite deformations ϵ_2, which form a complete set, i.e.

$$\int d\epsilon_2 |\epsilon_2\rangle\langle\,\epsilon_2| = 1, \tag{2}$$

then the amplitude for the system to have deformation ϵ_2 can be written as

$$g(\epsilon_2) = \langle\epsilon_2|\Psi\rangle\,. \tag{3}$$

$g(\epsilon_2)$ can be understood as the wave function in the so-called *deformation representation*. Inserting Eq. (1) into Eq. (3) leads to

$$g(\epsilon_2) = \int d\epsilon_2' f(\epsilon_2')\,\langle\epsilon_2|\psi(\epsilon_2')\rangle\,. \tag{4}$$

$\left\langle\epsilon_2|\psi(\epsilon_2')\right\rangle$ in (4) must satisfy

$$\begin{aligned}&\int d\epsilon_2''\,\langle\psi(\epsilon_2)|\epsilon_2''\rangle\,\langle\epsilon_2''|\psi(\epsilon_2')\rangle\\ &= \langle\psi(\epsilon_2)|\psi(\epsilon_2')\rangle\\ &= \Pi(\epsilon_2,\epsilon_2'),\end{aligned} \tag{5}$$

where $\Pi(\epsilon_2,\epsilon_2')$ is the norm in the Hill-Wheeler equation [15]. Now the problem is to find an expression for $\left\langle\epsilon_2|\psi(\epsilon_2')\right\rangle$. In the process of solving the Hill-Wheeler equation, $\Pi(\epsilon_2,\epsilon_2')$ should be diagonalized:

$$\int d\epsilon_2'\Pi(\epsilon_2,\epsilon_2')u_k(\epsilon_2') = n_k u_k(\epsilon_2). \tag{6}$$

If we define

$$\Pi^{1/2}(\epsilon_2,\epsilon_2') = \sum_k u_k(\epsilon_2)\,\sqrt{n_k}\,u_k^*(\epsilon_2'), \tag{7}$$

we are able to show that $\Pi^{1/2}(\epsilon_2,\epsilon_2')$ satisfies Eq. (5). Therefore we can use the quantity $|g(\epsilon_2)|^2$ to represent the probability of the system having deformation ϵ_2.

3 Extension of the projected shell model

The Projected Shell Model (PSM) [14] has been successful in the microscopic description of the yrast properties of rotational nuclei and high-spin bands with multi-quasiparticle (qp) structures. For those studies one usually starts with a fixed deformation of the mean-field (with either axial or triaxial symmetry), and the dynamics is obtained through mixing various qp configurations preserving the symmetries. The studied structures are associated with the rotational motion. For a description of vibrations, however, the original PSM [14] has not been successful. In order to apply PSM to the low-lying collective vibrations, the model has to be extended to allow the mixing of product states with different deformations.

As in the original PSM one superimposes qp-states with good symmetries, we take projected states associated with different axial deformation, ϵ_2, and write Eq. (1) as

$$\left|\Psi^{I,N}\right\rangle = \int d\epsilon_2 f^{I,N}(\epsilon_2)\hat{P}^I\hat{P}^N\,|\Phi_0(\epsilon_2)\rangle\,, \tag{8}$$

where $\hat{P}^I$ and $\hat{P}^N$ are the projection operators on good angular momentum and particle number, restoring the rotational symmetry violated in the deformed mean-field and the gauge symmetry violated in the BCS approximation. $|\Phi_0(\epsilon_2)\rangle$ in (8) is a Nilsson+BCS state, i.e. the qp vacuum with deformation ϵ_2. For each ϵ_2, a set of Nilsson single-particle states can be generated, with the Nilsson parameter κ, μ taken from Ref. [16].

We use discrete values for ϵ_2, with the bin value $\Delta\epsilon_2 = 0.050$. The number of the deformation mesh points ranges from 7 to 14, depending on the convergence of the results. With the discrete generator coordinates, the Hill-Wheeler equation becomes

$$\sum_j \{\left\langle\Phi(\epsilon_{2i})|H\hat{P}|\Phi(\epsilon_{2j})\right\rangle - E_i\left\langle\Phi(\epsilon_{2i})|\hat{P}|\Phi(\epsilon_{2j})\right\rangle\} f(\epsilon_{2j}) = 0. \tag{9}$$

The Hamiltonian in Eq. (9) is the same as those used for usual PSM calculations [14]

$$H = H_0 - \frac{\chi}{2}\sum_\mu Q_\mu^+ Q_\mu - G_M P^+P - G_Q\sum_\mu P_\mu^+ P_\mu. \tag{10}$$

In the usual PSM calculations, the strength of the quadrupole-quadrupole interaction χ is determined self-consistently with the quadrupole deformation ϵ_2 [14]. As we now have different deformations, we use in the present work a fixed χ corresponding to $\epsilon_2 = 0.305$. The monopole pairing strengths are taken to be $G_M = (G_1 \mp G_2(N - Z)/A)/A$, with minus sign for neutrons and plus sign for protons. Here we use $G_1 = 21.24$ MeV and $G_2 = 13.86$ MeV, as given by Ref. [14]. The strength of the quadrupole pairing is taken to be $G_Q = 0.2G_M$. For all of the presented results we use the same set of parameters.

4 Results and discussions

For the Gd isotopes with $A = 150 - 160$, corresponding to neutron numbers $N = 86 - 96$, the total energy curves are

presented in Fig. 1 as functions of the quadrupole deformation parameter ϵ_2. Here the energy refers to the expectation value of the Hamiltonian operator in the projected Nilsson+BCS state with a specific deformation. In Fig. 1 one can see that for ^{150,152}Gd, the minimum of the energy curves corresponds to vary small values of ϵ_2, suggesting that these nuclei are near spherical. For the isotopes with $A \geq 156$, the minima of the curves locate at larger deformation values ($\epsilon_2 > 0.3$), indicating that they are deformed. It is evident that a widely-distributed, flat-bottom curve is found for ^{154}Gd, which is understood as having a transitional behavior [17]. Thus our calculated energy curves suggest that ^{154}Gd lies at the critical point of the shape phase transition, in agreement with the observation that the shape phase transition happens around the neutron number $N = 90$.

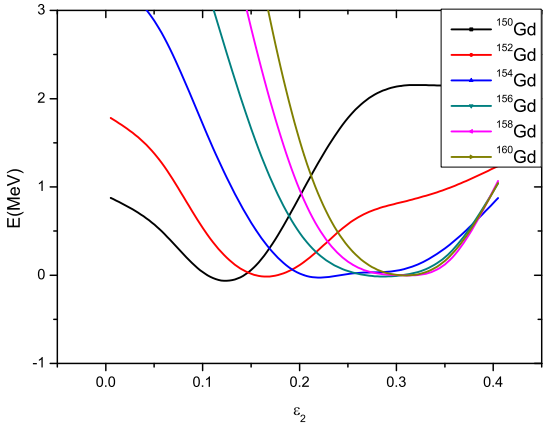

Figure 1. (Color online) Calculated energy curves for $^{150-160}$Gd as functions of quadrupole deformation ϵ_2.

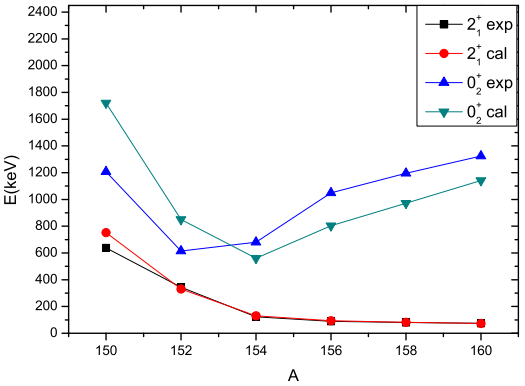

Figure 2. (Color online) Comparison of calculated first 2^+ state and second 0^+ state for $^{150-160}$Gd with the experimental data, taken from Refs. [18–23].

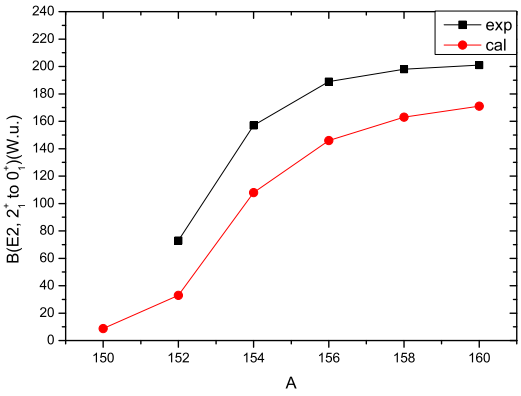

Figure 3. (Color online) Comparison of calculated $B(E2)$ values from the first 2^+ state to the ground state for $^{150-160}$Gd with the experimental data, taken from www.nndc.bnl.gov.

For a proper description of transition nuclei, we should not only consider the deformation at the energy minimum, but also other deformations near it. To do so we have to solve the Hill-Wheeler equation (9). The eigenvalues obtained for the first 2^+ states and the second 0^+ states are given in Fig. 2. It can be seen that the lowering of the first 2^+ states with increasing neutron number is well reproduced by the calculation. Note that the calculations for different isotopes are performed with the same set of parameters, and therefore, the results in Fig. 2 have demonstrated that our calculation can describe the onset of deformation in a natural manner. It can also be found in Fig. 2 that the calculated excitation energies of the second 0^+ states are also in reasonable agreement with the experimental data. Besides the excitation energies, the calculated $B(E2)$ values for transitions from the first 2^+ state to the ground state shown in Fig. 3 are also well in coincidence with data. These $B(E2)$ values are calculated with the effective charges $e^\pi = 1.5e$ and $e^\nu = 0.5e$, the standard values used in previous PSM calculations. The small $B(E2)$ values for ^{150,152}Gd are signatures of a near-spherical shape of these nuclei. On the other hand, the large $B(E2)$ values of ^{158,160}Gd suggest a typical rotational behavior, which indicates that these isotopes have large quadrupole deformation. The increase of $B(E2)$ values with neutron number indicates the onset of deformation.

There is another experimental indicator for the onset of deformation: the energy ratio $R_{42} = E(4^+_1)/E(2^+_1)$. For vibrational nuclei (spherical) one has $R_{42} \sim 2.0$. For well deformed nuclei with a rotational spectrum $E(I) \propto I(I+1)$, one has $R_{42} \sim 3.33$. At the critical point of shape phase transition, which is described by the $X(5)$ dynamical symmetry, one has $R_{42} \sim 3.0$ [10]. It is seen in Fig. 4 that R_{42} is indeed close to 2.0 for ^{150}Gd and to 3.33 for $^{156-160}$Gd. For ^{154}Gd, R_{42} is approximately 3.0, which suggests that along the isotopic chain, the location of the critical point lies at ^{154}Gd with $N = 90$.

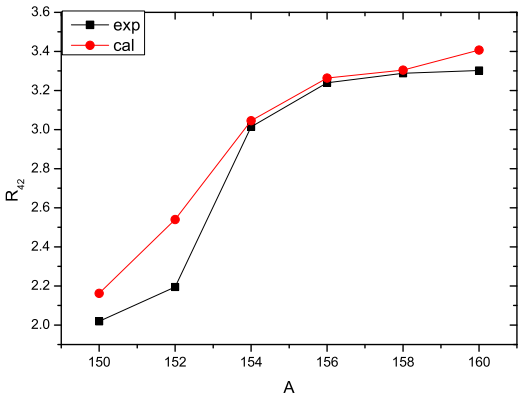

Figure 4. (Color online) Comparison of calculated energy ratio $E(4_1^+)/E(2_1^+)$ for $^{150-160}$Gd with the experimental ones.

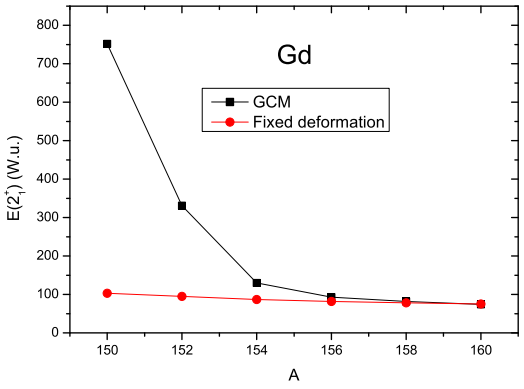

Figure 5. (Color online) Comparison of two calculations for the first 2^+ energy for $^{150-160}$Gd: black squares corresponding to the full GCM calculation and red dots to the calculation with a fixed deformation.

As indicated in Eq. (8), the GCM wave functions superimpose the symmetry-conserved states with different deformations. This is important particularly for nuclei lying in the transitional region where no definite shape can be associated with them. The effect of performing the GCM type of calculation for those "soft" nuclei can be clearly seen in Figs. 5 and 6. In these two figures, results from two calculations are presented. Black squares correspond to the full GCM calculation using Eq. (8) as the trail wave function and red dots to the usual PSM calculation with assumption of a fixed deformation for each nucleus. It can be easily concluded from the figures that for well-deformed nuclei such as ^{156,158,160}Gd, there are no much differences between the results of the two calculations, meaning that the original PSM [14] is a good approximation to the general GCM treatment for well-deformed nuclei. However, qualitative differences in the two calculations are seen for the light isotopes. The much higher 2^+ excitation energy and much smaller $B(E2)$ transitions for ^{150,152,154}Gd (see the experimental data in Figs. 2 and 3) can only be described by the full GCM treatment. It is not possible that a fixed-deformation approach can describe the transitional properties of the first 2^+ energy level and its transition to the ground state.

The results presented above show that the GCM calculations using deformation ϵ_2 as the generator coordinate can provide a reasonable description for the phase transition region observed in these Gd isotopes. It is now of great interest to further explore whether the obtained wave functions can tell us something more about the intrinsic structure of the isotopic chain. We show the wave function distribution in the deformation representation (Eq. (**??**)) for two representative isotopes ^{154}Gd and ^{160}Gd. Calculated $g(\epsilon_2)$ values for ^{154,160}Gd are shown in Fig. 7. It is seen that the curve for the first 0^+ state is Gaussian-like, while the functions $g(\epsilon_2)$ for the second and the third 0^+ state oscillate. The second 0^+ state has one and the third 0^+ state has two nodes. These forms remind us

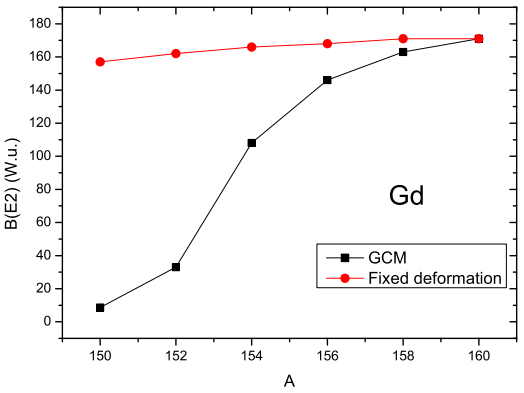

Figure 6. (Color online) Comparison of two calculations for $B(E2)$ transitions from the first 2^+ state to the ground state for $^{150-160}$Gd: black squares corresponding to the full GCM calculation and red dots to the calculation with a fixed deformation.

to results of a one-dimensional harmonic oscillator, with some anharmonicities as discussed below. The first three 0^+ states shown here correspond to the ground state, one-phonon state, and two-phonon state, respectively, in a one-dimensional harmonic oscillator potential characterized by the coordinate ϵ_2.

Normalized probability distribution function $g^2(\epsilon_2)$ for the ground state 0_1^+ and the excited 0_2^+ state are shown in Fig. 8. For the 0_1^+ state, it exhibits, as expected, a beautiful Gaussian shape centered at the minimum of the energy surface, where the ground-state deformation may be defined. The deformation can be directly read from the figure as $\epsilon_2 = 0.25$ for ^{154}Gd and $\epsilon_2 = 0.30$ for ^{160}Gd, respectively. It is seen that the distribution is wider for ^{154}Gd, reflecting the softness of this nucleus. Quite differently, $g^2(\epsilon_2)$ for

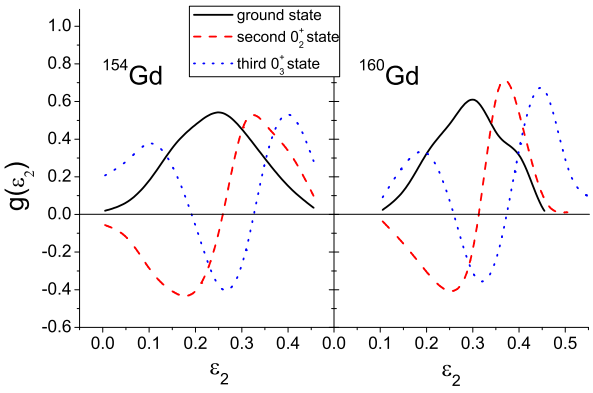

Figure 7. (Color online) Calculated distribution function of deformation for the first three 0^+ states in ^{154}Gd and ^{160}Gd. This figure is taken from Fig. 3 of Ref. [24].

the 0_2^+ state are much extended, with a distribution minimum, instead of a maximum, at the ground-state deformation. The dip in the 0_2^+ state corresponds to a node in $g(\epsilon_2)$ in Fig. 7. There is not one, but two separate peaks in the $g^2(\epsilon_2)$ curve corresponding to the enhanced probability at the turning points of the oscillation. Obviously, the distribution in deformation for the 0_2^+ states is much more fragmented, reflecting a vibrational nature of these states.

The distribution function $g^2(\epsilon_2)$ describes the probability that the nucleus has the deformation ϵ_2. The picture shown in Fig. 8 clearly distinguishes the two 0^+ states. While for the 0_1^+ ground state, the system stays mainly at system's deformation with the largest probability, such a probability for the 0_2^+ state is very small. For the 0_2^+ state, that the two peaks having different heights lie separately at both sides of the equilibrium indicates an anharmonic oscillation. Our calculation suggests a stronger anharmonicity for the excited 0_2^+ state in the strongly-deformed ^{160}Gd. The anharmonicity increases with neutron number

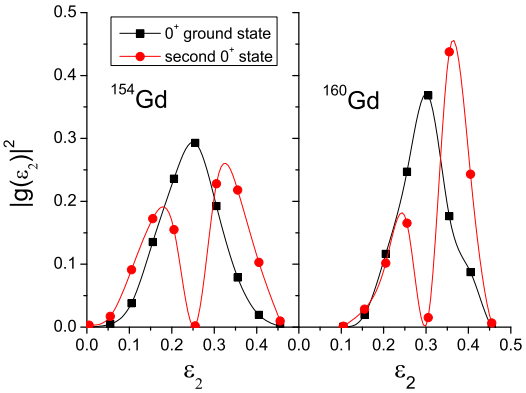

Figure 8. (Color online) Calculated probability function of deformation for the ground state 0_1^+ and the excited 0_2^+ state in ^{154}Gd and ^{160}Gd. Symbols correspond to the discrete deformations used for the integration in Eq. (8). This figure is taken from Fig. 4 of Ref. [24].

because of the increasing excitation energy, where the potential deviates more from an ideal quadratic shape of the harmonic oscillator. Interestingly, the system prefers to have a larger probability in the site of larger deformation, as the peak height at $\epsilon_2 \approx 0.38$ is obviously higher. Moreover, the distance from a peak to the equilibrium measures the average deviation from the equilibrium. The fact that the distance is larger for ^{154}Gd indicates again the softness of this isotope.

It should be pointed out that the present work does not intend to suggest the nature of the excited 0^+ state, which has been a debating question [25, 26]. A final answer to this question requires a microscopic model that can incorporate all the competing aspects. In the first place, such a model must be able to provide quantitative explanations for the observations [27, 28] before conclusions can be drawn.

5 Summary

The present work describes a step of going beyond the original projected shell model to build many-body wave functions as a superposition of symmetry-conserved states with different quadrupole deformations ϵ_2. We have discussed how to incorporate the idea of the generate coordinate method that allows interpretation of the wave functions in the deformation representation. We have shown, by taking the $N = 86 - 96$ isotopes of $^{150-160}$Gd as examples, that with the same set of parameters, the observed transitional behavior is reasonably reproduced by our microscopic calculation. It has been found that these states exhibit clear features of quantum oscillations, with large fluctuations in deformation found for soft nuclei and strong anharmonicities for rigidly-deformed nuclei. With a single set of parameters, the characteristic features of qualitatively different systems can be distinguished by the resulting distribution functions, thus providing some microscopic insight for the traditional collective states in nuclei.

6 Acknowledgment

Valuable discussions with P. Ring and G. Bertsch are acknowledged. This work was supported by the National Natural Science Foundation of China (Nos. 11135005 and 11075103) and by the 973 Program of China (No. 2013CB834401).

References

[1] A. Bohr, B. R. Mottelson, *Nuclear Structure*, Vol. 2 (Benjamin, New York, 1975)

[2] K. Heyde, J. L. Wood, Rev. Mod. Phys. **83**, 1467 (2011)

[3] P. J. Nolan, P. J. Twin, Ann. Rev. Nucl. Part. Sci., **38**, 533 (1988)

[4] Y. Sun, J.-y. Zhang, G.-L. Long, C.-L. Wu, Chin. Sci. Bull. **54**(3), 358 (2009)

[5] A. N. Andreyev *et al.*, Nature **405**, 430 (2000)
[6] Y. Sun, M. Wiescher, A. Aprahamian, and J. Fisker, Nucl. Phys. A **758**, 765 (2005)
[7] P. H. Regan *et al.*, Phys. Rev. Lett. **90**, 152502 (2003)
[8] Y. Sun, P. M. Walker, F.-R. Xu, Y.-X. Liu, Phys. Lett. B **659**, 165 (2008)
[9] A. D. Ayangeakaa *et al.*, Phys. Rev. Lett. **110**, 102501 (2013)
[10] F. Iachello, Phys. Rev. Lett. **87**, 052502 (2001)
[11] F. Iachello, A. Arima, *The Interacting Boson Model* (Cambridge University Press, Cambridge, England, 1987)
[12] P. Cejnar, J. Jolie, Phys. Rev. E **61**, 6237 (2000)
[13] T. Niksic, D. Vretenar, G. A. Lalazissis, P. Ring, Phys. Rev. Lett. **99**, 092502 (2007)
[14] K. Hara and Y. Sun, Int. J. Mod. Phys. E **4**, 637 (1995)
[15] D. J. Hill and J. A. Wheeler, Phys. Rev. **89** (1953) 1102.
[16] S. G. Nilsson, Mat. Fys. Medd. Dan. Vidensk. Selsk **29**, no. 16 (1955)
[17] P. Cejnar, J. Jolie, R. F. Casten, Rev. Mod. Phys. **82**, 2155 (2010)
[18] E. Dermateosian, J. K. Tuli, Nuclear Data Sheets **75**, 827 (1995)
[19] Agda Artna-Cohen, Nucl. Dat. Sheets **79** (1996) 1
[20] C. W. Reich, Nucl. Dat. Sheets **110** (2009) 2257
[21] C. W. Reich, Nucl. Dat. Sheets **99** (203) 753
[22] R. G. Helmer, Nucl. Dat. Sheets **101** (2004) 325
[23] C. W. Reich, Nucl. Dat. Sheets **105** (2005) 557
[24] F.-Q. Chen, Y. Sun, P. Ring, Phys. Rev. C, in press
[25] P. E. Garrett, J. Phys. G **27**, R1 (2007)
[26] J. L. Wood, J. Phys. Conf. Ser. **403**, 012011 (2012)
[27] W. D. Kulp, *et al.*, Phys. Rev. Lett. **91**, 102501 (2003); Phys. Rev. C **71**, 041303(R) (2005); Phys. Rev. C **77**, 061301(R) (2008)
[28] J. F. Sharpey-Schafer *et al.*, Eur. Phys. J. A **47**, 5 (2011); **47**, 6 (2011)